ACE2 Receptor Decoy is a Potent Prophylactic and Therapeutic for SARS-CoV-2

Takuya Tada[1,†], Belinda M. Dcosta[1,†], Hao Zhou[1] and Nathaniel R. Landau[1]#

Affiliation:

[1]Department of Microbiology, NYU Grossman School of Medicine, New York, NY, USA.

[†] These authors have contributed equally to this work.

#Corresponding author:

Nathaniel R. Landau, Ph.D.

NYU Grossman School of Medicine

430 East 29th Street, Alexandria West Building, Rm 509, New York, NY 10016

Email: nathaniel.landau@med.nyu.edu

Phone: (212) 263-9197

Summary

The emergence of SARS-CoV-2 variants with highly mutated spike proteins has presented a major obstacle to the use of monoclonal antibodies for the prevention of SARS-CoV-2 infection and treatment of COVID-19. Better prophylactic and therapeutics for current and future variants are needed. We show that a high affinity receptor decoy protein in which a modified ectodomain of human ACE2 is fused a single domain of an immunoglobulin heavy chain Fc region dramatically suppressed virus loads in mice upon challenge with high dose of parental SARS-CoV-2 or Omicron variants BA.1 and BA.2 and potently suppressed virus replication when administered post-infection. The approach offers protection that is broader than monoclonal antibodies that are likely to be evaded by the continued evolution of the viral spike protein.

Introduction

Since the initial zoonosis of SARS-CoV-2 into humans, the virus has undergone rapid evolutionary adaptation to the new host with the appearance of variants with divergent spike proteins. The appearance of the first variants of concern (Alpha, Beta, Gamma and Delta), each with a few mutations in the receptor binding domain, were replaced by the sudden emergence of the highly divergent Omicron variant first reported in Botswana and South Africa (2022). As the virus has continued to adapt to its human host, it has become increasingly transmissible as a result of mutations that increase the affinity of the spike protein for the ACE2 receptor. Omicron BA.1 rapidly became prevalent world-wide and then gave rise to the BA.2 subvariant (2022) and most recently additional highly transmissible subvariants BA.2.12.1, BA.4, BA.5 with spike proteins that are further increased for ACE2 affinity (Cao et al., 2022).

The divergence of the spike protein has presented a major obstacle both to the effectiveness of vaccines and to monoclonal antibody therapy. The Regeneron REGN-COV-2 monoclonal antibody cocktail and Lilly monoclonal antibodies that had been highly effective at preventing hospitalization and morbidity of patients infected by the earlier variants of concern (VOCs) (Baum et al., 2020; Chen et al., 2021a; Chen et al., 2021b; Hansel et al., 2010; Planas et al., 2021b; Tada et al., 2021a; Tada et al., 2022b; Tada et al., 2021b; Tada et al., 2022c; Wang et al., 2021; Weinreich et al., 2021; Weisblum et al., 2020), were rendered ineffective by the heavily mutated spikes of the Omicron variants which escape neutralization (Cameroni et al., 2021; Cao et al., 2021; Hoffmann et al., 2021; Iketani et al., 2022; Liu et al., 2022; Planas et al., 2021a; Tada et al., 2022a; VanBlargan et al., 2022; Zhou et al., 2022). The Omicron variants pose an additional obstacle to the prophylactic use of monoclonal antibodies (Cameroni et al., 2021; Cao et al., 2021; Hoffmann et al., 2021; Iketani et al., 2022; Liu et al., 2022; Planas et al., 2021a; Tada et al., 2022a; VanBlargan et al., 2022; Zhou et al., 2022). The AstraZeneca dual monoclonal antibody cocktail Evusheld is used primarily for prophylaxis in immunocompromised individuals for whom

55 vaccination may be ineffective (ClinicalTrials.gov); however, both Evusheld antibodies have
56 significantly decreased neutralizing titers against the BA.1 and BA.2 variants which could affect
57 the long-term effectiveness of the therapy (Cao et al., 2021; Iketani et al., 2022; Liu et al., 2022;
58 Planas et al., 2021a; Tada et al., 2022a; Zhou et al., 2022). The Sotrovimab monoclonal antibody
59 Vir-7831 retains activity against the earlier VOCs but has substantially decreased neutralizing titer
60 against the BA.1 and BA.2 variants. Currently, the only monoclonal antibody that neutralizes the
61 Omicron variants with high titer is LY-CoV1404 (Westendorf et al., 2022). In light of the resistance
62 of the Omicron variants to neutralization by therapeutic monoclonal antibodies, there is a need
63 for improved treatment and therapies that are effective against the current variants and that are
64 less affected by the variability of the viral spike protein.
65
66 The concept of decoy receptors for the treatment of virus infection was initially tried as a therapy
67 for HIV infection. Decoys are predicted to be less susceptible to escape by mutagenesis of the
68 viral spike protein and less like to induce an antibody response as they are derived from self-
69 protein sequences to which the immune system is tolerant. A soluble CD4 “immunoadhesin”, in
70 which the ectodomain of CD4 was fused to an immunoglobulin domain was previously reported
71 (Traunecker et al., 1989). Although the protein neutralized the virus by binding the gp120 subunit
72 of the viral envelope glycoprotein *in vitro* (Daar et al., 1990; Haim et al., 2009; Orloff et al., 1993;
73 Schenten et al., 1999; Sullivan et al., 1998), it failed to decrease virus loads when used to treat
74 patients. More recently the concept was revived using an adeno-associated virus vector
75 expressing an enhanced soluble eCD4-Ig decoy (Gardner et al., 2015; Spitsin et al., 2020).
76 Rhesus macaques treated with the vector were highly protected against a challenge with SHIV-
77 AD8 and SIVmac239 (Gardner et al., 2015; Spitsin et al., 2020).
78
79 We previously reported on a receptor decoy protein for SARS-CoV-2 termed a “microbody” in
80 which the ACE2 ectodomain is fused to the CH3 domain of an immunoglobulin IgG1 heavy chain

81 (Tada et al., 2020). Truncation of the Fc domain served to decrease the mass of the protein as
82 well as to prevent binding of the protein to cell surface Fcγ receptors (Maute et al., 2015). The
83 ACE2 ectodomain contained a point mutation (H345A) that inactivates the carboxypeptidase
84 activity of ACE2 (Guy et al., 2005) to prevent possible effects of the protein on blood pressure.
85 The protein potently neutralized the parental D614G virus and viruses with the variant of concern
86 spike proteins by binding to the viral spike protein, preventing association of the virus with cell
87 surface ACE2 (Tada et al., 2020). Because ACE2 binding is a conserved feature of all SARS-
88 CoV-2 spike proteins, the decoy is predicted to maintain its neutralizing activity against current,
89 as well as future virus variants, without being affected by mutations in the variant spike proteins.
90 Several groups have recently reported on similar ACE2.Fc receptor decoys. Hoshino's group
91 reported that an ACE2.Fc fusion protein containing mutations A25V, K31N and N90H
92 administered 2 hours post-infection increased the survival in the hamster model (Higuchi et al.,
93 2021; Ikemura et al., 2022). Zhang *et al.* reported that a high affinity receptor decoy termed
94 sACE2v2.4.Fc fusion protein containing mutations T27Y, L79T, and N330Y (Chan et al., 2020)
95 protected K18-ACE2 transgenic mice from infection with SARS-CoV-2 variant and protected mice
96 from disease when given 12- and 24-hours post-infection (Zhang et al., 2022).
97
98 In this report, we tested a decoy protein mutated to increase its affinity for the spike protein for its
99 ability to prevent and treat SARS-CoV-2 infection in mouse models. We found that the
100 recombinant decoy protein was a potent prophylactic against both parental SARS-CoV-2 and the
101 Omicron variant and a therapeutic that rapidly and dramatically decrease virus load.

102 ## Results

103 **High affinity decoy inhibits SARS-CoV-2 infection and replication *in vitro*.**

104 We previously reported the construction of plasmid vectors expressing an ACE2 microbody
105 (pcACE2.mb) in which the ectodomain of human ACE2 is fused to the IgG1 CH3 domain and
106 soluble ACE2 (pcsACE2) that encodes the unfused ectodomain (Tada et al., 2020). To further
107 increase the potency of the microbody decoy protein, we induced the mutations
108 T27Y/L79T/N330Y reported by Chan *et al.* (Chan et al., 2020) that increase ACE2 affinity for the
109 SARS-CoV-2 spike protein (pcACE2.1mb) (**Figure. 1A**). In addition, the proteins are mutated in
110 the catalytic active site at position 345 (H345A) to inactivate phosphohydrolase activity (Guy et
111 al., 2005), preventing possible effects on blood pressure, and contain a carboxy-terminal His-Tag
112 (**Figure. 1B**). The decoy proteins were produced by transfection of ExpiCHO cells with the
113 expression vectors and then purified by affinity chromatography and size exclusion
114 chromatography (**Figure. 1C**). The antiviral activity of the decoy proteins was tested in the
115 pseudotyped lentivirus neutralization assay. The results show that the ACE2.mb decoy
116 neutralized virus with the D614 spike protein with a potency 10-fold increase compared to sACE2
117 while the high affinity ACE2.1mb decoy increased neutralizing activity another 5-fold (**Figure. 1D**).
118 The decoy neutralized virus with the D614G spike with a similar potency. The high affinity
119 ACE2.1mb decoy was also highly active against virus with the Alpha, Beta, Gamma and Delta
120 spike proteins. Analysis of decoy antiviral activity against live virus showed that the decoys
121 suppressed the replication of USA-WA1/2020 and the Omicron variants. The ACE2.1mb decoy
122 was 35-fold and 4-fold more potent than sACE2 and the ACE2.1mb, respectively (**Figure. 1E**).
123 The decoys were active against BA.1 and BA.2 although the variants showed a degree of
124 resistance with a 6.2-fold and 16-fold decreased titer, respectively.

125

126 Avidity of the decoys for the spike protein was analyzed in two assays (Tada et al., 2020; Tada et
127 al., 2022b). The first was a virion binding assay that measured the binding of spike protein-

128 pseudotyped virions to bead-bound decoy protein. The results showed that the ACE2.1mb decoy
129 bound more avidly to virions than sACE2 or the ACE2.1mb (**Supplementary Figure 1A**). The
130 second assay measured the binding of sACE2-NLuc, ACE2.mb-NLuc, ACE2.1mb-NLuc
131 decoy:nanoluciferase fusion proteins to bind to spike protein-expressing 293T cells
132 (**Supplementary Figure 1B and C**). The results confirmed the increased avidity of ACE2.1mb
133 compared to sACE2 and ACE2.mb for spike protein binding and showed the increased potency
134 of the decoy for the Alpha, Beta, Gamma and Delta spikes and a minor 4- and 5.9-fold decrease
135 in binding to BA.1 and BA.2 spike proteins (**Supplementary Figure 1D**). Taken together, the
136 results showed that the ACE2.1mb decoy protein was a potent inhibitor of parental and variant
137 SARS-CoV-2.
138
139 **Increased half-life of microbody decoy *in vivo*.**
140 Fusion of Fc domains onto proteins has been used to increase their half-life *in vivo* (Czajkowsky
141 et al., 2012; Roopenian and Akilesh, 2007). To determine whether the truncated single IgG1 CH3
142 domain of the microbody decoy would extend its half-life and to determine the tissue localization
143 of the decoy, sACE2- nanoluciferase (NLuc) and ACE2.1mb-NLuc fusion proteins were injected
144 i.p and the mice were live-imaged over 3 days. The results showed that the proteins localized
145 mainly to the spleen and that the sACE2 decoy was nearly undetectable after one day, the
146 ACE2.1mb protein was detectable after 3 days (**Figure 2A**). To further analyze the tissue
147 distribution of the ACE2.1mb-NLuc decoy and to understand how the route of administration
148 affects its distribution, The ACE2.1mb decoy was injected intraperitoneally (i.p.) or intravenously
149 (i.v.) or instilled intranasally (i.n.) and 72 hrs post-administration, the amount of decoy protein in
150 different tissues was determined by measuring the luciferase activity in lysates of individual
151 organs. In mice injected i.p, the decoy localized mainly to the spleen, liver and serum with a minor
152 fraction in the lung. I.v. injection similarly localized the decoy to the spleen, liver and serum but
153 resulted in a 100-fold increase in localization to the lung. I.n. instillation resulted in localization of

154 the decoy to the lung and trachea, as might be expected, with a small amount of the protein in
155 the nasal tissues and serum (**Figure 2B**). To determine the half-life of the decoy *in vivo*, the
156 ACE2.1mb decoy was administered i.v. or i.n. and luciferase activity in the serum and lung was
157 measured over 15 days. The half-life of the i.v. injected or i.n. instilled decoy in the serum was
158 5.2 and 5.1 days, respectively. In the lung, the half-life of the i.v. injected protein was 4.0 days
159 and i.n. instilled protein was 7.6 days (**Figure 2C**). The increased half-life and localization to the
160 lung by the i.n. instilled protein suggests that this route of administration would be most effective
161 therapeutically while i.v. injection would also be effective.
162
163 **Decoy protects from SARS-CoV-2 infection.**
164 To test the ability of the high affinity decoy to prevent SARS-CoV-2 infection *in vivo*, hACE2-Tg
165 mice that have a knock-in of human ACE2 (Zhou et al., 2021) were administered 100 μg of
166 ACE2.1mb protein by i.p. or i.v. injection or i.n. instillation. One day later, the mice were
167 challenged with a high dose of SARS-COV-2 USA-WA1/2020. For comparison, the mice were
168 treated in parallel with the REGN-CoV2 cocktail, a mixture of REGN10933 and REGN10987 that
169 has been shown to potently suppress SARS-CoV-2 replication in animal models (Baum et al.,
170 2020). Viral RNA in the lung was quantified 3-dpi., the day of at which virus loads peak (Bao et
171 al., 2020). The decoy strongly suppressed virus replication in the mice when administered either
172 i.v. or i.n. Injection of the decoy i.p decreased the virus load 108-fold compared to mock while i.v
173 injection decreased the virus load 15,700-fold and i.n. instillation decreased the virus load 26,500-
174 fold, a level at which the viral RNA could not be undetected (**Figure 3A and B**). The monoclonal
175 antibody cocktail closely mirrored the effect of the decoy protein in the three routes of
176 administration. To compare the effectiveness of the sACE2, ACE2.mb, ACE2.1mb decoys, the
177 proteins were injected i.v. and the mice were challenged with live virus. The results showed that
178 sACE2 was the least effective while the ACE2.1mb decoy caused the greatest decrease in virus
179 load (**Figure 3C**). Histological examination of the lung tissue of the mice showed a prominent

180 infiltration of immune cells in the untreated mice (**Figure 3D)** that was largely absent in mice
181 treated with sACE2 and completely prevented by treatment with the ACE2.1mb decoy. To
182 understand the kinetics with which the decoy protein suppressed virus replication, mice were
183 treated and then infected 24 hours later and viral RNA was measured every day over the course
184 of one week. The results showed the absence of detectable viral RNA in the lung over the time
185 course except for a small blip at 3-days post-injection (dpi); virus was not detected in the trachea
186 over the time course (**Figure 3E**). A dose-response analysis of the potency of the decoy
187 administered i.v. and i.n. showed that 100 μg of the protein suppressed virus replication to
188 undetectable levels and that as little as 10 μg suppressed virus replication 12-fold
189 **(Supplementary Figure 2A)**; administration i.n. was slightly more effective than i.v. at the 50 and
190 10 microgram doses. A dose-response analysis of the REGN-COV2 cocktail showed that the
191 potency of the decoy was similar to that of the cocktail administered i.v or i.n. **(Supplementary**
192 **Figure 2B).**
193
194 The efficacy of the decoy against the Omicron variants was tested in BALB/c mice which support
195 high levels of replication of the virus (Halfmann et al., 2022). As controls, the mice were treated
196 with the LY-CoV1404 monoclonal antibody which is active against the Omicron variant (Iketani et
197 al., 2022; Liu et al., 2022; Tada et al., 2022a) or with the REGN-COV2 cocktail which is inactive
198 against Omicron (Cameroni et al., 2021; Cao et al., 2021; Hoffmann et al., 2021; Iketani et al.,
199 2022; Liu et al., 2022; Planas et al., 2021a; Tada et al., 2022a; VanBlargan et al., 2022). The
200 following day, the mice were challenged with BA.1 or BA.2 virus. The decoy decreased the BA.1
201 virus load 56-fold by i.v. injection and BA.2,100-fold by i.n. instillation. The decreases were
202 comparable to that caused by LY-CoV1404 (**Figure 3F, left**). The REGN-COV2 cocktail had no
203 effect. The decoy was also active against BA.2. The decrease in virus load was not as dramatic
204 but was similar to that of the highly potent LY-CoV1404 at the same dose (**Figure 3F, right and**
205 **Supplementary Figure 2B)**. The durability of protection was analyzed by administering the decoy

206 at increasing times pre-infection. The results showed a high degree of protection when the decoy
207 was administered up to 2 days prior to infection and a moderate degree of protection 3-dpi (200-
208 fold decrease in virus load); the protection was lost 5-dpi (**Figure 3G)**.
209
210 **Decoy suppresses virus load following SARS-CoV-2 infection.**
211 To determine whether the decoy could be used to treat an established infection, hACE2-Tg mice
212 were infected with USA-WA1/2020 and then treated 1-, 6-, 12- and 16-hours later injected i.p., i.v.
213 or instilled i.n. with the ACE2.1mb decoy or REGN-COV2 cocktail (**Figure 4A**). At 3-dpi, virus
214 loads in the lung were measured. I.p. injection of the decoy or monoclonal antibody had no effect
215 on virus load at any of the time points (**Figure 4B**). In contrast, 1-hour post-infection, the i.v.
216 injected decoy decreased the virus load 1,100-fold while i.n. instillation decreased the virus load
217 27,500-fold to an undetectable level. Virus loads were similarly decreased when the decoy was
218 administered 6 hours post-infection. At 12 hours post-infection, the i.v. injected decoy had no
219 significant effect while the i.n. instilled decoy decreased the virus load 20-fold, an effect that was
220 maintained at the 16-hour time point. The effect of the decoy was comparable to that of the REGN-
221 SARS-COV-2 cocktail at all time points. The effect of the decoy was not as pronounced on
222 Omicron BA.1 or BA.2 with decreases of 290-fold and 30-fold, respectively for the i.n. instilled
223 decoy (**Figure 4C**). The effect of the decoy was 4-50-fold higher than LY-CoV1404 (**Figure 4C**).

224 **Discussion**

225 We report here that a high affinity microbody decoy was highly effective both in the form of a
226 recombinant protein for the treatment of SARS-CoV-2 infection. The decoy was highly potent *in*
227 *vitro* against viruses with VOC spike proteins including Omicron BA.1 and BA.2. I.v. injection or
228 i.n. instillation of the recombinant decoy protein prior to infection protected human ACE2
229 transgenic mice from a high dose of live virus, suppressing virus replication to undetectable levels
230 and preventing lung pathology. Administration of the recombinant protein shortly after infection
231 with SARS-CoV-2 rapidly suppressed virus replication in the lung. The decoy was at least as
232 potent for prophylaxis and treatment as the highly potent emergency use authorized monoclonal
233 antibodies. The addition of the single CH3 IgG1 domain served to extend the protein's half-life
234 and increased its avidity for the spike protein while preventing absorbance of the protein to Fc
235 receptors that would decrease the concentration of the free protein (Chen et al., 2020; Maute et
236 al., 2015).

237

238 I.v. injection or i.n. instillation of the decoy protein 1- or 6-hours after infection with USA-WA1/2020
239 decreased the virus load 10,000-fold, demonstrating the potency with which it suppresses virus
240 replication. Administration at later times (12- and 16-hours post-infection) was less effective,
241 decreasing virus loads by 100-fold. This timing should not be taken to mean that in humans the
242 therapy would need to be administered that soon post-infection as the mouse does not accurately
243 model the kinetics of virus replication in humans where peak virus loads occur 3-5 days following
244 the appearance of symptoms (Jones et al., 2021), a considerably slower disease course than in
245 the mouse. In our study, the effects of the decoy were very similar to those of the therapeutic
246 monoclonal antibodies which are highly effective at preventing hospitalization and death when
247 given during the symptomatic phase of infection, several days post-infection (Group et al., 2021;
248 Razonable et al., 2021). The decoy is likely to act in humans with kinetics similar to that of anti-
249 spike protein monoclonal antibodies that neutralize virus by a similar mechanism. Results

250 reported here with the recombinant protein are consistent with those previously reported with a
251 high affinity decoy 3N39v2 containing 4 mutations (Higuchi et al., 2021; Ikemura et al., 2022) and
252 with the decoy sACE2v2.4-Ig that showed protection against infection and disease in hamsters
253 and transgenic mouse models.
254
255 The route of administration of the decoy influenced its antiviral effects. I.p. injection of the decoy,
256 which localized the protein mainly to the liver, serum and spleen, was not effective, as was the
257 case for i.p. injected monoclonal antibody. I.v. injection resulted in a much higher concentration
258 in the lung and potent antiviral activity. I.n. instillation localized the decoy primarily to the lung and
259 trachea, as might be expected, and provided in the strongest degree of protection. The findings
260 suggest that the decoy acts in the lung to suppress virus replication and that both i.v and i.n. are
261 effective routes of administration.
262
263 The decoy was less protective against the BA.1 and BA.2 subvariants both *in vitro* and *in vivo*
264 than against the parental USA-WA1/2020 virus. Its activity against the variants was comparable
265 to that of the highly potent therapeutic monoclonal antibody LY-CoV1404, suggesting that the
266 decoy will be similarly effective against the variants in clinical use. The decreased titer of the
267 decoy against the variants suggest that its affinity for the spike protein could be further optimized
268 by screening for mutations that increase its affinity for the Omicron protein.
269
270 The rapid evolution of SARS-CoV-2 has presented a major obstacle to the development of
271 effective therapies targeted to the spike protein. *In vitro* selection studies suggest that the spike
272 protein is destined to continue to evolve over the next several years imposing further challenge
273 to the development of broadly neutralizing monoclonal antibodies (Schmidt et al., 2021). The
274 receptor decoy approach has the advantage that it is much more resistant to evasion in the face
275 of novel variants as the spike protein needs to preserve its affinity for ACE2, leaving variants with

276 novel spike protein mutations susceptible to neutralization. In fact, as the virus has continued to
277 evolve and increase its transmissibility following zoonosis into humans, the variant spike proteins
278 have tended to increase their affinity for ACE2, resulting in increased sensitivity to neutralization
279 by the decoy. It is conceivable that a variant will emerge that switches its receptor usage to an
280 alternative cell surface protein, thereby becoming resistant to the decoy. Such an event has not
281 occurred in nature and extensive laboratory mutagenesis of the spike protein has not resulted in
282 a receptor switch (Greaney et al., 2021; Starr et al., 2020). If such a switch were to occur in a
283 pandemic coronavirus or virus of another virus class, a receptor decoy could be developed based
284 on its receptor and rapidly deployed.
285
286 **Limitations of Study**
287 The study is based on analyses of decoy receptor in ACE2 transgenic mice. While these mice
288 express human ACE2 at physiological levels in the appropriate tissues, they may not entirely
289 accurately reflect the human. Calculations of how much protein would be required to treat humans
290 may not be accurate. Moreover, the time course of SARS-CoV-2 infection is longer in humans,
291 and thus the time courses analyzed here may not be directly translatable to human.
292
293 **Acknowledgements**
294 We thank Meike Dittman and Bruno Rodriguez-Rodriguez for ACE2.TMPRSS2.Vero E6 cells and
295 Victor Torres and Juliana Ilmain (NYU Grossman School of Medicine) for assistance with FPLC
296 purification of recombinant proteins. We thank members of the Experimental Pathology Research
297 Laboratory which is supported by NIH Grant P30CA016087 to the NYU Langone Laura and Isaac
298 Perlmutter Cancer Center for histology. The work was funded by grants from the NIH to N.R.L.
299 (DA046100, AI122390 and AI120898). T.T. was supported by the Vilcek/Goldfarb Fellowship
300 Endowment Fund.
301

302 **Author contributions**

303 T.T., B.M.D. and H.Z. conducted the experiments. T.T. designed the experiments and wrote the
304 paper. T.T. and B.M.D. did the statistical analysis. N.R.L. supervised the study and revised the
305 manuscript.

306

307 **Declaration of Interests**.

308 The authors declare no competing interests.

309 **Figure Legend**

310 **Figure. 1. High affinity ACE2 decoy potently neutralizes SARS-CoV-2 variants.**

311 (A) The domain structure of soluble ACE2, ACE2mb and high affinity ACE2.1mb is shown. The
312 ectodomain is shaded green; transmembrane domain (TM), intracytoplasmic domain (IC), the
313 IgG1 CH3 domain is indicated and carboxy-terminal 6XHis-tag are shown. The high affinity
314 ACE2.1mb decoy has mutations to increase spike protein affinity (T27Y, L79T, N330Y) and
315 activate site point mutation H345A to inactivate carboxypeptidase activity. The genes are cloned
316 into expression vector pcDNA3.1 in which transcription is driven by the cytomegalovirus promoter.
317 (B) The 3D structure of the ACE2 (green) and spike protein (purple) complex was generated
318 using PyMoL. The position of the mutations for improved decoy in the ACE2 carboxypeptidase
319 domain are shown.
320 (C) Recombinant decoy proteins produced in transfected ExpiCHO cells were purified by Ni-NTA
321 affinity chromatography followed by size-exclusion chromatography. Purity of the proteins (25μg)
322 were analyzed on a silver staining.
323 (D) Neutralizing activity of the decoy proteins was measured using the variant spike protein-
324 pseudotyped lentiviruses assay with a packaged luciferase expressing lentiviral genome.
325 Lentiviruses were pseudotyped by the ancestral spike, parental spike or Alpha, Beta, Gamma and
326 Delta spike protein. Vesicular stomatitis virus G protein (VSV-G) pseudotype served as a
327 specificity control. Variable amounts of decoy (indicated on the X-axis) were incubated with a
328 fixed amount of pseudotyped lentivirus (MOI=0.2). Infectivity (indicated on the Y-axis) is displayed
329 as the percent infection normalized to control untreated virus as determined by luciferase assay
330 of the infected cultures. The IC50s (nM) of decoy neutralization on each variant spike protein
331 pseudotyped virus is calculated using the neutralization curves is shown in the table below.
332 (E) 2-fold serial dilutions of decoy proteins were incubated with USA-WA1/2020, Omicron BA.1
333 or BA.2 virus (MOI=0.01) and added to Vero E6. After 2 days of infection, cells were harvested
334 and subgenomic E gene was quantified by RT-PCR. IC50s (nM) were calculated from curves

335 using Prism GraphPad 8 software and shown in the table. The experiment was done three times
336 with similar results.
337
338 **Figure. 2. ACE2.1mb is stable *in vivo*.**
339 (A) C57BL/6 mice were injected i.p. with 100 μg of sACE2.NLuc or ACE2.1mb.NLuc
340 nanoluciferase fusion proteins. After 6, 12, 24, 48 and 72 hours of injection, the mice were imaged
341 with Nano-Glo substrate. The panel on the right shows a graph of the fluorescence in relative light
342 units (RLU).
343 (B) ACE2.1mb-NLuc (100 μg) was administered i.p., i.v. or i.n. to C57/BL6 mice (n=3). Three days
344 post injection (dpi), nasal epithelium, lung, trachea, spleen, thymus, liver and serum were
345 harvested and luciferase activity was quantified.
346 (C) ACE2.1mb-NLuc protein (100 μg) was administered by i.v. injection or i.n. installation. After
347 0.25, 1, 7, 10, 21 days, lungs and serum were harvested and luciferase activity was quantified.
348 The concentration and half-life of decoy was determined based on standard curve obtained from
349 the mixture of serial diluted ACE2.1mb-NLuc proteins and tissue lysate from wild-type (n=3). The
350 experiment was done twice with similar results.
351
352 **Figure. 3. ACE2 decoy protects mice from SARS-CoV-2 infection and decreases virus**
353 **loads.**
354 (A) Experimental scheme for decoy prophylaxis is shown. hACE2-Tg or BALB/c mice were
355 injected i.p., i.v. or i.n. with 100 μg of ACE2.1mb or REGN-COV2 or LY-CoV1404. One day post
356 injection, the mice were challenged with 1 X 10^4 PFU of SARS-CoV-2 USA-WA1/2020 (hACE2
357 Tg) or SARS-CoV-2 Omicron BA.1 or BA.2 (BALB/c) and viral RNA copies were quantified 2
358 (Omicron) or 3 days (WA1/2020) post-infection.
359 (B) Viral RNA copies (WA1/2020) in lung were quantified -dpi.

360 (C) sACE2, ACE2.mb or ACE2.1mb proteins (100 μg) was administered to hACE2-Tg mice (n=5)
361 by i.n. instillation. The following day, the mice were challenged with 1 X 10^4 PFU of SARS-CoV-2
362 USA-WA1/2020. 3 dpi, subgenomic viral E RNA in the lung was quantified by RT-qPCR.
363 (D) Hematoxylin and eosin (HE) staining of lung sections from SARS-CoV-2 WA1/2020 infected
364 mice. Mice were injected with sACE2, ACE2.1mb. Post 1 day of injection, mice were challenged
365 with SARS-CoV-2. 3-dpi, lung histology was visualized with HE staining. Scale bars, 200 μm (top),
366 50 μm (bottom).
367 (E) ACE2.1mb protein (100 μg) was administered to hACE2-Tg- mice (n=4) by i.n. instillation and
368 the following day, challenged with 1 X 10^4 PFU of SARS-CoV-2 USA-WA1/2020. At 1-, 2-, 3-, 4-,
369 5-, 6- and 7-dpi, subgenomic viral E gene RNA in the lung and trachea were quantified. The
370 horizontal line indicates the level of detection determined using uninfected mouse tissues.
371 (F) BALB/c mice were injected i.v. or i.n. with 100 μg of ACE2.1mb or LY-CoV1404 antibody (n=4-
372 5). One day post injection, the mice were challenged with 1 X 10^4 PFU Omicron BA.1 (left) or
373 BA.2 (right). Two days post-infection, lung subgenomic viral E RNA was quantified by RT-PCR.
374 The copy numbers detected in uninfected samples is the result of low level background priming.
375 Confidence intervals are shown as the mean ± SD. **P ≤ 0.01, ***P≤0.001, ****P≤0.0001. The
376 experiment was done twice with similar results.
377 (G) hACE2-Tg mice were instlled i.n. with 100 μg of decoy proteins and then infected 0, 0.25, 1,
378 3, 5, and 7 days later with SARS-CoV-2 WA1/2020. At 3-dpi, lung subgenomic viral E RNA was
379 quantified by RT-qPCR.
380
381 **Figure. 4. ACE2 decoy treats SARS-CoV-2 infection and decreases virus loads in mice.**
382 (A) Therapeutic experimental scheme for decoy treatment is shown. hACE2-Tg were infected with
383 USA-WA1/2020 virus (n=4-5) and BALB/c mice were infected with Omicron BA.1 or BA.2 virus
384 via i.n. injection. After 1, 6, 12, 16 hours post infection, mice were treated with 100μg ACE2.1mb

385 or REGN-COV2 or LY-CoV1404 via i.p., i.v. or i.n. injection. Viral RNA copies in lung were
386 quantified 2 (Omicron) or 3 days (WA1/2020) post-infection. The copy numbers detected in
387 uninfected samples is the result of low level background priming.
388 (B) After 1, 6, 12, 16 hours post infection, mice were treated with decoy. Viral RNA copies
389 (WA1/2020) in lung were quantified -dpi.
390 (C) After 6 hours post infection, mice were treated with decoy. Viral RNA copies (Omicron BA.1
391 (left) or BA.2 (right)) in lung were quantified 2-dpi. Confidence intervals are shown as the mean ±
392 SD. **P ≤ 0.01, ***P≤0.001, ****P≤0.0001. The experiment was done twice with similar results.

STAR Methods

Resource Availability

Lead Contact

Further information and requests for resources and reagents should be directed to and will be fulfilled by the Lead Contact, Nathaniel R. Landau (nathaniel.landau@med.nyu.edu).

Materials Availability

All unique DNA constructs, proteins and pseudotyped virus generated in this study are available from the Lead Contact upon request.

Data and Code Availability

- The data used in this study are available upon request from the lead contact.
- This paper does not report original code.
- Any additional information required to reanalyze the data reported in this paper is available from the lead contact upon request.

Experimental Model and Subject Details

Mice

hACE2-Tg (B6.129S2(Cg)ACE2tm1(ACE2)Dwnt/J) and BALB/c mice were purchased from the Jackson Laboratory. We collected as many mice as possible and used them for the experiments. The sample size was described in the Figure legend. All animal experiments were done under protocols approved by the NYU Langone Institutional Animal Care and Use Committee (#170304) in accord with the standards set by the Animal Welfare Act. The study was approved by the NYU School of Medicine Division of Comparative Medicine Standard Operating Protocol (40-008-17). All experiments were done twice or triplicates with similar results.

419 **Cells**

420 293T and Vero E6 cells were cultured at 37°C under 5% CO_2 in Dulbecco's modified Eagle
421 medium (DMEM) supplemented with 10% fetal bovine serum (FBS) and penicillin/streptomycin.
422 ACE2.293T(Tada et al., 2020) and ACE2.TMPRSS2.Vero E6 cells were cultured with the addition
423 of puromycin (1 μg/ml). ExpiCHO-S cells (Thermo Fisher Scientific) were grown at 37 °C under
424 8% CO_2 in suspension in ExpiCHO serum-free expression medium in a shaking incubator.

425

426 **Plasmids**

427 The plasmids pLenti.GFP.NLuc, pMDL, pcRev, pcCOV2.S.delta19 and pcCOV2.S.delta19-
428 variant spikes used to produce spike protein-pseudotyped lentiviruses have been previously
429 described (Tada et al., 2020). The decoy expression vectors pcsACE2, pcACE2mb and
430 pcACE2.H345A.mb have been previously described (Tada et al., 2020). To construct the
431 expression vector pcACE2.1mb encoding the high affinity microbody decoy ACE2.1mb, point
432 mutations T27Y, L79T, N330Y were introduced into pcACE2.H345A.mb by overlap extension
433 PCR and the amplicon was cloned into the Kpn-I and Xho-I sites of pcDNA6. To construct the
434 expression vector pcsACE2-NLuc and pcsACE2.1mb-NLuc expressing a decoy:nanoluciferase
435 protein, DNA fragments encoding ACE2 amino acids 1-741 and nanoluciferase were amplified by
436 PCR and joined by overlap extension PCR using primers containing Kpn-I and Xho-I sites. The
437 resulting amplicon was cloned into Kpn-I and Xho-I cleaved pcDNA6. Nucleotide sequences of
438 all plasmids were confirmed by DNA sequencing.

439

440 **Monoclonal antibodies**

441 REGN-COV2 (REGN10933+REGN10987) were provided by Regeneron Pharmaceuticals.
442 Bebletovimab (LY-CoV1404) was obtained from discarded vials.

443

444 **Recombinant protein purification**

445 ExpiCHO-S cells (Thermo Fisher Scientific) cultured in shaker flasks in serum-free medium were
446 grown to a density of 6 X 10^6/ml and transfected with 400 μg of plasmid DNA using with 1.28 ml
447 of ExpiFectamine. After 12 hours, 2.4 ml of ExpiCHO Enhancer and 64 ml of ExpiCHO Feed were
448 added. After 4 days, the culture supernatant was collected and passed over a 0.22 μm filter. The
449 supernatant was passed over a 5 ml HiTrap Chelating column charged with nickel on an Akta
450 FPLC (GE healthcare). The column was washed with buffer containing 20 mM Tris pH 8, 150 mM
451 NaCl, 10mM imidazole and the bound protein was then eluted in buffer containing 250 mM
452 imidazole. The eluate was loaded onto a Superdex 200 size-exclusion column (GE healthcare) in
453 running buffer containing 10 mM Tris pH 7.4, 150 mM NaCl. Fractions were collected and those
454 containing peak protein concentrations were pooled. Protein purity was analyzed on a 4-12% Bis-
455 Tris SDS-PAGE by silver staining (Invitrogen).
456
457 **Method Details**
458 **Virion-decoy pull-down assay**
459 Decoy proteins (5, 2, 0.5 and 0.1 μg) were allowed to bind 30 μl of nickel-nitrilotriacetic acid-
460 agarose beads (QIAGEN) for 1 hour after which unbound decoy was removed by washing with
461 PBS. The beads were then incubated with 30 μl (30 μg) of D614G spike protein-pseudotyped
462 virus for 1 hour after which unbound virions were removed by washing with PBS. The bound
463 virions were then eluted from the beads with Laemmle loading buffer containing reducing agent
464 (Invitrogen) and analyzed on an immunoblot probed with anti-p24 monoclinal antibody AG3.0
465 (Creative Biolabs) and horseradish peroxidase (HRP)-conjugated goat anti-mouse IgG secondary
466 antibody (Sigma-Aldrich). The signals were developed with Luminata Crescendo Western HRP
467 Substrate (Millipore) and membranes were visualized on an iBright imaging system (Invitrogen)
468 (Tada et al., 2020).
469

470 **Cell-based decoy spike binding assay**

471 293T cells (2 x 10^6) were transfected with 2 μg spike expression vector by lipofection using
472 lipofectamine 2000 (Invitrogen). One day post-transfection, the cells were plated in a 96 well plate
473 at 1 X 10^4 cells/well. The following day, decoy-NLuc fusion protein was added to the wells. After
474 30 minutes, the free fusion protein was removed by washing with PBS and cell-bound luciferase
475 activity was measured using NanoGlo luciferase substrate (Nanolight) in an Envision 2103
476 microplate luminometer (PerkinElmer) (Tada et al., 2022b).

477

478 **Pseudotyped lentiviral neutralization assay**

479 Spike protein-pseudotyped lentiviruses were generated as previously described (Tada et al.,
480 2020). Briefly, virus stocks were generated by cotransfection of 293T cells with pMDL,
481 pLenti.GFP.nLuc, pcCoV2.S-Δ19 and pRSV.Rev using the calcium phosphate method. After 2
482 days, the culture supernatant was harvested and the virus was concentrated by ultracentrifugation
483 at 4°C for 1 hour at 30,000 X g and normalized for reverse transcriptase (RT) activity. To
484 determine the neutralizing titer of the decoy proteins, serially diluted decoys were incubated with
485 pseudotyped virus (MOI=0.2) for 30 minutes at room temperature and then added to ACE2.293T
486 or ACE2.TMPRSS2.Vero E6 cells. At 2-dpi, luminescence was measured in an Envision 2103
487 microplate luminometer (PerkinElmer). All samples were assayed in duplicate and IC50s were
488 calculate by Prism 8 software.

489

490 **Decoy localization *in vivo***

491 100 μg of ACE2.1mb-NLuc or sACE2-NLuc proteins were injected intraperitoneal (i.p.),
492 intravenous (i.v.) or by intranasal (i.n.) instillation. After 6, 12, 24, 48, 72 hours, the mice were
493 sacrificed and the tissues were homogenized in lysing matrix D tubes (MP Biomedicals) with a
494 FastPrep-24 5G homogenizer (MP Biomedicals). Blood was collected by submandibular bleeding

495 and serum was harvested. The tissue lysates were mixed with an equal volume of Nano-GLO
496 Luciferase Assay Reagent (Nanolight) and luciferase activity was quantified on an Envision 2103
497 plate reader (PerkinElmer). Decoy concentration and half-life were determined based on a
498 standard curve derived from the mixture of serial diluted ACE2.1mb-NLuc proteins and tissue
499 lysate from wild-type. For live imaging of the decoy, mice were injected i.p. with 100 µl 1:40 diluted
500 Nano-GLO substrate. After 3 minutes, the mice were live imaged on an IVIS Lumina III XR
501 (PerkinElmer).
502
503 **Preparation of live virus**
504 SARS-CoV-2 WA1/2020 P1 virus stock (BEI Resources, NR-52281) was amplified by a second
505 round of replication on Vero E6 cells infected at MOI=0.01. At 3-dpi, the culture medium was
506 harvested, filtered through a 0.45 μm filter and frozen at -80°C in aliquots. The virus was titered
507 by plaque assay on Vero E6 cells (Wei et al., 2020). SARS-CoV-2 Omicron BA.1 (BEI Resources,
508 NR56461) and BA.2 stocks (BEI Resources, NR-56781) were grown on ACE2.TMPRSS2.Vero
509 E6 cells infected at an MOI=0.1. The P1 stock was amplified by a second round of replication on
510 ACE2.TMPRSS2.Vero E6 cells infected at MOI=0.01. The virus-containing supernatant was
511 filtered through a 0.45 μm filter, concentrated by passage through an Amicon filter (Millipore) and
512 stored in aliquots at -80°C. The virus was titered by plaque assay on Vero E6 cells. Live virus was
513 handled by trained personnel in a Biosafety level 3 facility.
514
515 **Prophylaxis and treatment of mice with decoy proteins**
516 For prophylaxis, 6-8 weeks old hACE2-Tg or BALB/c mice were anesthetized with isoflurane and
517 injected i.v. with decoy or monoclonal antibody, or alternatively, were anesthetized with ketamine–
518 xylazine cocktail and administered the proteins by i.n. instillation. After 1 day, the mice were
519 infected i.n. with 2.0 X 10^4 PFU USA-WA1/2020 (hACE2-Tg) or Omicron BA.1 or Omicron BA.2
520 (BALB/c). At 2-dpi for Omicron-infected mice or 3-dpi for USA-WA1/2020-infected mice, the mice

521 were sacrificed and lungs and trachea were harvested and homogenized. Littermate controls
522 were included in all experiments. RNA was prepared from 200 µl of the lysate using the Quick-
523 RNA MiniPrep kit (Zymo Research). For treatment experiments, hACE2-Tg mice were infected
524 with 2.0 X 10^4 PFU of SARS-CoV-2 USA-WA1/2020 i.n. At 1-, 6-, 12- or 16-hours post-infection,
525 mice were administered therapeutic monoclonal antibodies or decoy protein (100 µg) i.p., i.v. or
526 i.n. Three days post-infection, lung and trachea were harvested and SARS-CoV-2 subgenomic E
527 gene levels were quantified by RT-qPCR.
528
529 **RT-qPCR**
530 Virus loads were measured by quantification of subgenomic viral E gene by RT-qPCR with
531 TaqMan probes. Cellular RNA was mixed with TaqMan Fast Virus 1-step Master Mix (Applied
532 Biosystems), 10 mM forward and reverse primers and 2 mM probe. PCR cycles were 95°C for
533 20s, 95°C for 3s, 40 cycles at 60°C for 30s) using forward primer E Sarbeco F
534 (ACAGGTACGTTAATAGTTAATAGCGT), reverse primer E Sarbeco R
535 (ATATTGCAGCAGTACGCACACA) and probe E Sarbeco P1(FAM-
536 ACACTAGCCATCCTTACTGCGCTTCG-BHQ1) (Corman et al., 2020). E gene subgenomic RNA
537 copies were measured using forward primer subgenomic F (CGATCTCTTGTAGATCTGTTCTC)
538 (Emma S. Winkler, 2022), reverse primer E Sarbeco R and probe E Sarbeco P1). Absolute copy
539 numbers were determined by normalization to a standard curve generated with *in vitro* transcribed
540 synthetic RNA containing the E gene sequence (2019-nCoV_E Positive Control, IDT: 10006896).
541 Cell lysate GAPDH copy numbers were measured as a control using mGAPDH.forward
542 (CAATGTGTCCGTCGTGGATCT) and mGAPDH.reverse (GTCCTCAGTGTAGCCCAAGATG)
543 with mGAPDH probe (CGTGCCGCCTGGAGAAACCTGCC). Data from tissue analyses was
544 normalized to GAPDH. Virus load was determined by the 2−ΔΔCTmethod).
545
546 **Histology**

547 Mice were infected with USA-WA1/2020 and sacrificed 3-dpi. Tissues were fixed in 10% buffered
548 formalin and processed through graded ethanol and xylene solutions and then embedded in
549 paraffin with a Leica Peloris automated processor. Five-micron sections were deparaffinized and
550 stained with hematoxylin and eosin on a Leica ST5020 automated histochemical stainer. The
551 slides were scanned at 40X on a Leica AT2 whole slide scanner.
552
553 **Data analysis and statistics**
554 All experiments were in technical duplicates or triplicates. Statistical significance was determined
555 by the two-tailed, unpaired t test using GraphPad Prism (Version 8) software. Significance was
556 based on two-sided testing. Confidence intervals are shown as the mean ± SD. (*P≤ 0.05, **P≤
557 0.01, ***P≤0.001, ****P≤0.0001).

558 **References**

559 Bao, L., Deng, W., Huang, B., Gao, H., Liu, J., Ren, L., Wei, Q., Yu, P., Xu, Y., Qi, F.*, et al.*
560 (2020). The pathogenicity of SARS-CoV-2 in hACE2 transgenic mice. Nature *583*, 830-833.
561 Baum, A., Ajithdoss, D., Copin, R., Zhou, A., Lanza, K., Negron, N., Ni, M., Wei, Y.,
562 Mohammadi, K., Musser, B.*, et al.* (2020). REGN-COV2 antibodies prevent and treat SARS-
563 CoV-2 infection in rhesus macaques and hamsters. Science *370*, 1110-1115.
564 Cameroni, E., Bowen, J.E., Rosen, L.E., Saliba, C., Zepeda, S.K., Culap, K., Pinto, D.,
565 VanBlargan, L.A., De Marco, A., di Iulio, J.*, et al.* (2021). Broadly neutralizing antibodies
566 overcome SARS-CoV-2 Omicron antigenic shift. Nature.
567 Cao, Y., Wang, J., Jian, F., Xiao, T., Song, W., Yisimayi, A., Huang, W., Li, Q., Wang, P., An,
568 R.*, et al.* (2021). Omicron escapes the majority of existing SARS-CoV-2 neutralizing antibodies.
569 Nature.
570 Cao, Y., Yisimayi, A., Jian, F., Song, W., Xiao, T., Wang, L., Du, S., Wang, J., Li, Q., Chen, X.*,*
571 *et al.* (2022). BA.2.12.1, BA.4 and BA.5 escape antibodies elicited by Omicron infection. Nature.
572 CDC (2022). Omicron Variant: What You Need to Know.
573 Chan, K.K., Dorosky, D., Sharma, P., Abbasi, S.A., Dye, J.M., Kranz, D.M., Herbert, A.S., and
574 Procko, E. (2020). Engineering human ACE2 to optimize binding to the spike protein of SARS
575 coronavirus 2. Science *369*, 1261-1265.
576 Chen, R.E., Winkler, E.S., Case, J.B., Aziati, I.D., Bricker, T.L., Joshi, A., Darling, T.L., Ying, B.,
577 Errico, J.M., Shrihari, S.*, et al.* (2021a). In vivo monoclonal antibody efficacy against SARS-
578 CoV-2 variant strains. Nature *596*, 103-108.
579 Chen, R.E., Zhang, X., Case, J.B., Winkler, E.S., Liu, Y., VanBlargan, L.A., Liu, J., Errico, J.M.,
580 Xie, X., Suryadevara, N.*, et al.* (2021b). Resistance of SARS-CoV-2 variants to neutralization by
581 monoclonal and serum-derived polyclonal antibodies. Nat Med.

582 Chen, S., Chen, S., Lian, G., Li, Y., Ye, X., Zou, J., Li, R., Tan, Y., Li, X., Zhang, M., *et al.*
583 (2020). Development and validation of a novel nomogram for pretreatment prediction of liver
584 metastasis in pancreatic cancer. Cancer Med *9*, 2971-2980.
585 ClinicalTrials.gov phase III Double-blind, Placebo-controlled Study of AZD7442 for Pre-
586 exposure Prophylaxis of COVID-19 in Adult. (PROVENT).
587 Czajkowsky, D.M., Hu, J., Shao, Z., and Pleass, R.J. (2012). Fc-fusion proteins: new
588 developments and future perspectives. EMBO Mol Med *4*, 1015-1028.
589 Daar, E.S., Li, X.L., Moudgil, T., and Ho, D.D. (1990). High concentrations of recombinant
590 soluble CD4 are required to neutralize primary human immunodeficiency virus type 1 isolates.
591 Proc Natl Acad Sci U S A *87*, 6574-6578.
592 Gardner, M.R., Kattenhorn, L.M., Kondur, H.R., von Schaewen, M., Dorfman, T., Chiang, J.J.,
593 Haworth, K.G., Decker, J.M., Alpert, M.D., Bailey, C.C., *et al.* (2015). AAV-expressed eCD4-Ig
594 provides durable protection from multiple SHIV challenges. Nature *519*, 87-91.
595 Greaney, A.J., Starr, T.N., Gilchuk, P., Zost, S.J., Binshtein, E., Loes, A.N., Hilton, S.K.,
596 Huddleston, J., Eguia, R., Crawford, K.H.D., *et al.* (2021). Complete Mapping of Mutations to the
597 SARS-CoV-2 Spike Receptor-Binding Domain that Escape Antibody Recognition. Cell Host
598 Microbe *29*, 44-57 e49.
599 Group, A.-T.L.-C.S., Lundgren, J.D., Grund, B., Barkauskas, C.E., Holland, T.L., Gottlieb, R.L.,
600 Sandkovsky, U., Brown, S.M., Knowlton, K.U., Self, W.H., *et al.* (2021). A Neutralizing
601 Monoclonal Antibody for Hospitalized Patients with Covid-19. N Engl J Med *384*, 905-914.
602 Guy, J.L., Jackson, R.M., Jensen, H.A., Hooper, N.M., and Turner, A.J. (2005). Identification of
603 critical active-site residues in angiotensin-converting enzyme-2 (ACE2) by site-directed
604 mutagenesis. FEBS J *272*, 3512-3520.
605 Haim, H., Si, Z., Madani, N., Wang, L., Courter, J.R., Princiotto, A., Kassa, A., DeGrace, M.,
606 McGee-Estrada, K., Mefford, M., *et al.* (2009). Soluble CD4 and CD4-mimetic compounds inhibit
607 HIV-1 infection by induction of a short-lived activated state. PLoS Pathog *5*, e1000360.

608 Halfmann, P.J., Iida, S., Iwatsuki-Horimoto, K., Maemura, T., Kiso, M., Scheaffer, S.M., Darling,
609 T.L., Joshi, A., Loeber, S., Singh, G.*, et al.* (2022). SARS-CoV-2 Omicron virus causes
610 attenuated disease in mice and hamsters. Nature *603*, 687-692.
611 Hansel, T.T., Kropshofer, H., Singer, T., Mitchell, J.A., and George, A.J. (2010). The safety and
612 side effects of monoclonal antibodies. Nat Rev Drug Discov *9*, 325-338.
613 Higuchi, Y., Suzuki, T., Arimori, T., Ikemura, N., Mihara, E., Kirita, Y., Ohgitani, E., Mazda, O.,
614 Motooka, D., Nakamura, S.*, et al.* (2021). Engineered ACE2 receptor therapy overcomes
615 mutational escape of SARS-CoV-2. Nature Communications *12*, 3802.
616 Hoffmann, M., Krüger, N., Schulz, S., Cossmann, A., Rocha, C., Kempf, A., Nehlmeier, I.,
617 Graichen, L., Moldenhauer, A.-S., Winkler, M.S.*, et al.* (2021). The Omicron variant is highly
618 resistant against antibody-mediated neutralization: Implications for control of the COVID-19
619 pandemic. Cell.
620 Ikemura, N., Taminishi, S., Inaba, T., Arimori, T., Motooka, D., Katoh, K., Kirita, Y., Higuchi, Y.,
621 Li, S., Suzuki, T.*, et al.* (2022). An engineered ACE2 decoy neutralizes the SARS-CoV-2
622 Omicron variant and confers protection against infection in vivo. Sci Transl Med *14*, eabn7737.
623 Iketani, S., Liu, L., Guo, Y., Liu, L., Chan, J.F.W., Huang, Y., Wang, M., Luo, Y., Yu, J., Chu, H.*,*
624 *et al.* (2022). Antibody evasion properties of SARS-CoV-2 Omicron sublineages. Nature *604*,
625 553-556.
626 Jones, T.C., Biele, G., Muhlemann, B., Veith, T., Schneider, J., Beheim-Schwarzbach, J.,
627 Bleicker, T., Tesch, J., Schmidt, M.L., Sander, L.E.*, et al.* (2021). Estimating infectiousness
628 throughout SARS-CoV-2 infection course. Science *373*.
629 Liu, L., Iketani, S., Guo, Y., Chan, J.F.W., Wang, M., Liu, L., Luo, Y., Chu, H., Huang, Y., Nair,
630 M.S.*, et al.* (2022). Striking antibody evasion manifested by the Omicron variant of SARS-CoV-
631 2. Nature *602*, 676-681.
632 Maute, R.L., Gordon, S.R., Mayer, A.T., McCracken, M.N., Natarajan, A., Ring, N.G., Kimura,
633 R., Tsai, J.M., Manglik, A., Kruse, A.C.*, et al.* (2015). Engineering high-affinity PD-1 variants for

634 optimized immunotherapy and immuno-PET imaging. Proc Natl Acad Sci U S A *112*, E6506-
635 6514.
636 Orloff, S.L., Kennedy, M.S., Belperron, A.A., Maddon, P.J., and McDougal, J.S. (1993). Two
637 mechanisms of soluble CD4 (sCD4)-mediated inhibition of human immunodeficiency virus type
638 1 (HIV-1) infectivity and their relation to primary HIV-1 isolates with reduced sensitivity to sCD4.
639 J Virol *67*, 1461-1471.
640 Planas, D., Saunders, N., Maes, P., Guivel-Benhassine, F., Planchais, C., Buchrieser, J.,
641 Bolland, W.-H., Porrot, F., Staropoli, I., Lemoine, F.*, et al.* (2021a). Considerable escape of
642 SARS-CoV-2 Omicron to antibody neutralization. Nature.
643 Planas, D., Veyer, D., Baidaliuk, A., Staropoli, I., Guivel-Benhassine, F., Rajah, M.M.,
644 Planchais, C., Porrot, F., Robillard, N., Puech, J.*, et al.* (2021b). Reduced sensitivity of SARS-
645 CoV-2 variant Delta to antibody neutralization. Nature *596*, 276-280.
646 Razonable, R.R., Pawlowski, C., O'Horo, J.C., Arndt, L.L., Arndt, R., Bierle, D.M., Borgen, M.D.,
647 Hanson, S.N., Hedin, M.C., Lenehan, P.*, et al.* (2021). Casirivimab-Imdevimab treatment is
648 associated with reduced rates of hospitalization among high-risk patients with mild to moderate
649 coronavirus disease-19. EClinicalMedicine *40*, 101102.
650 Roopenian, D.C., and Akilesh, S. (2007). FcRn: the neonatal Fc receptor comes of age. Nat
651 Rev Immunol *7*, 715-725.
652 Schenten, D., Marcon, L., Karlsson, G.B., Parolin, C., Kodama, T., Gerard, N., and Sodroski, J.
653 (1999). Effects of soluble CD4 on simian immunodeficiency virus infection of CD4-positive and
654 CD4-negative cells. J Virol *73*, 5373-5380.
655 Schmidt, F., Weisblum, Y., Rutkowska, M., Poston, D., DaSilva, J., Zhang, F., Bednarski, E.,
656 Cho, A., Schaefer-Babajew, D.J., Gaebler, C.*, et al.* (2021). High genetic barrier to SARS-CoV-2
657 polyclonal neutralizing antibody escape. Nature *600*, 512-516.
658 Spitsin, S., Schnepp, B.C., Connell, M.J., Liu, T., Dang, C.M., Pappa, V., Tustin, R., Kinder, A.,
659 Johnson, P.R., and Douglas, S.D. (2020). Protection against SIV in Rhesus Macaques Using

660 Albumin and CD4-Based Vector-Mediated Gene Transfer. Molecular therapy Methods & clinical
661 development *17*, 1088-1096.
662 Starr, T.N., Greaney, A.J., Hilton, S.K., Ellis, D., Crawford, K.H.D., Dingens, A.S., Navarro, M.J.,
663 Bowen, J.E., Tortorici, M.A., Walls, A.C.*, et al.* (2020). Deep Mutational Scanning of SARS-CoV-
664 2 Receptor Binding Domain Reveals Constraints on Folding and ACE2 Binding. Cell *182*, 1295-
665 1310 e1220.
666 Sullivan, N., Sun, Y., Binley, J., Lee, J., Barbas, C.F., 3rd, Parren, P.W., Burton, D.R., and
667 Sodroski, J. (1998). Determinants of human immunodeficiency virus type 1 envelope
668 glycoprotein activation by soluble CD4 and monoclonal antibodies. J Virol *72*, 6332-6338.
669 Tada, T., Dcosta, B.M., Samanovic, M.I., Herati, R.S., Cornelius, A., Zhou, H., Vaill, A.,
670 Kazmierski, W., Mulligan, M.J., and Landau, N.R. (2021a). Convalescent-Phase Sera and
671 Vaccine-Elicited Antibodies Largely Maintain Neutralizing Titer against Global SARS-CoV-2
672 Variant Spikes. mBio *12*, e0069621.
673 Tada, T., Fan, C., Chen, J.S., Kaur, R., Stapleford, K.A., Gristick, H., Dcosta, B.M., Wilen, C.B.,
674 Nimigean, C.M., and Landau, N.R. (2020). An ACE2 Microbody Containing a Single
675 Immunoglobulin Fc Domain Is a Potent Inhibitor of SARS-CoV-2. Cell Rep *33*, 108528.
676 Tada, T., Zhou, H., Dcosta, B.M., Samanovic, M.I., Chivukula, V., Herati, R.S., Hubbard, S.R.,
677 Mulligan, M.J., and Landau, N.R. (2022a). Increased resistance of SARS-CoV-2 Omicron
678 variant to neutralization by vaccine-elicited and therapeutic antibodies. EBioMedicine *78*,
679 103944.
680 Tada, T., Zhou, H., Dcosta, B.M., Samanovic, M.I., Cornelius, A., Herati, R.S., Mulligan, M.J.,
681 and Landau, N.R. (2022b). High-titer neutralization of Mu and C.1.2 SARS-CoV-2 variants by
682 vaccine-elicited antibodies of previously infected individuals. Cell Rep *38*, 110237.
683 Tada, T., Zhou, H., Dcosta, B.M., Samanovic, M.I., Mulligan, M.J., and Landau, N.R. (2021b).
684 Partial resistance of SARS-CoV-2 Delta variants to vaccine-elicited antibodies and convalescent
685 sera. iScience *24*, 103341.

686 Tada, T., Zhou, H., Samanovic, M.I., Dcosta, B.M., Cornelius, A., Herati, R.S., Mulligan, M.J.,
687 and Landau, N.R. (2022c). Neutralization of SARS-CoV-2 Variants by mRNA and Adenoviral
688 Vector Vaccine-Elicited Antibodies. Front Immunol *13*, 797589.
689 Traunecker, A., Schneider, J., Kiefer, H., and Karjalainen, K. (1989). Highly efficient
690 neutralization of HIV with recombinant CD4-immunoglobulin molecules. Nature *339*, 68-70.
691 VanBlargan, L.A., Errico, J.M., Halfmann, P.J., Zost, S.J., Crowe, J.E., Jr., Purcell, L.A.,
692 Kawaoka, Y., Corti, D., Fremont, D.H., and Diamond, M.S. (2022). An infectious SARS-CoV-2
693 B.1.1.529 Omicron virus escapes neutralization by therapeutic monoclonal antibodies. Nat Med.
694 Wang, P., Nair, M.S., Liu, L., Iketani, S., Luo, Y., Guo, Y., Wang, M., Yu, J., Zhang, B., Kwong,
695 P.D.*, et al.* (2021). Antibody resistance of SARS-CoV-2 variants B.1.351 and B.1.1.7. Nature
696 *593*, 130-135.
697 Weinreich, D.M., Sivapalasingam, S., Norton, T., Ali, S., Gao, H., Bhore, R., Musser, B.J., Soo,
698 Y., Rofail, D., Im, J.*, et al.* (2021). REGN-COV2, a Neutralizing Antibody Cocktail, in Outpatients
699 with Covid-19. N Engl J Med *384*, 238-251.
700 Weisblum, Y., Schmidt, F., Zhang, F., DaSilva, J., Poston, D., Lorenzi, J.C.C., Muecksch, F.,
701 Rutkowska, M., Hoffmann, H.-H., Michailidis, E.*, et al.* (2020). Escape from neutralizing
702 antibodies by SARS-CoV-2 spike protein variants. eLife *9*, e61312.
703 Westendorf, K., Zentelis, S., Wang, L., Foster, D., Vaillancourt, P., Wiggin, M., Lovett, E., van
704 der Lee, R., Hendle, J., Pustilnik, A.*, et al.* (2022). LY-CoV1404 (bebtelovimab) potently
705 neutralizes SARS-CoV-2 variants. Cell Rep *39*, 110812.
706 Zhang, L., Narayanan, K.K., Cooper, L., Chan, K.K., Skeeters, S.S., Devlin, C.A., Aguhob, A.,
707 Shirley, K., Rong, L., Rehman, J.*, et al.* (2022). An ACE2 decoy can be administered by
708 inhalation and potently targets omicron variants of SARS-CoV-2. EMBO Molecular Medicine *14*,
709 e16109.

710 Zhou, H., Dcosta, B.M., Landau, N.R., and Tada, T. (2022). Resistance of SARS-CoV-2
711 Omicron BA.1 and BA.2 Variants to Vaccine-Elicited Sera and Therapeutic Monoclonal
712 Antibodies. Viruses *14*.
713 Zhou, H., Dcosta, B.M., Samanovic, M.I., Mulligan, M.J., Landau, N.R., and Tada, T. (2021).
714 B.1.526 SARS-CoV-2 Variants Identified in New York City are Neutralized by Vaccine-Elicited
715 and Therapeutic Monoclonal Antibodies. mBio *12*, e0138621.
716

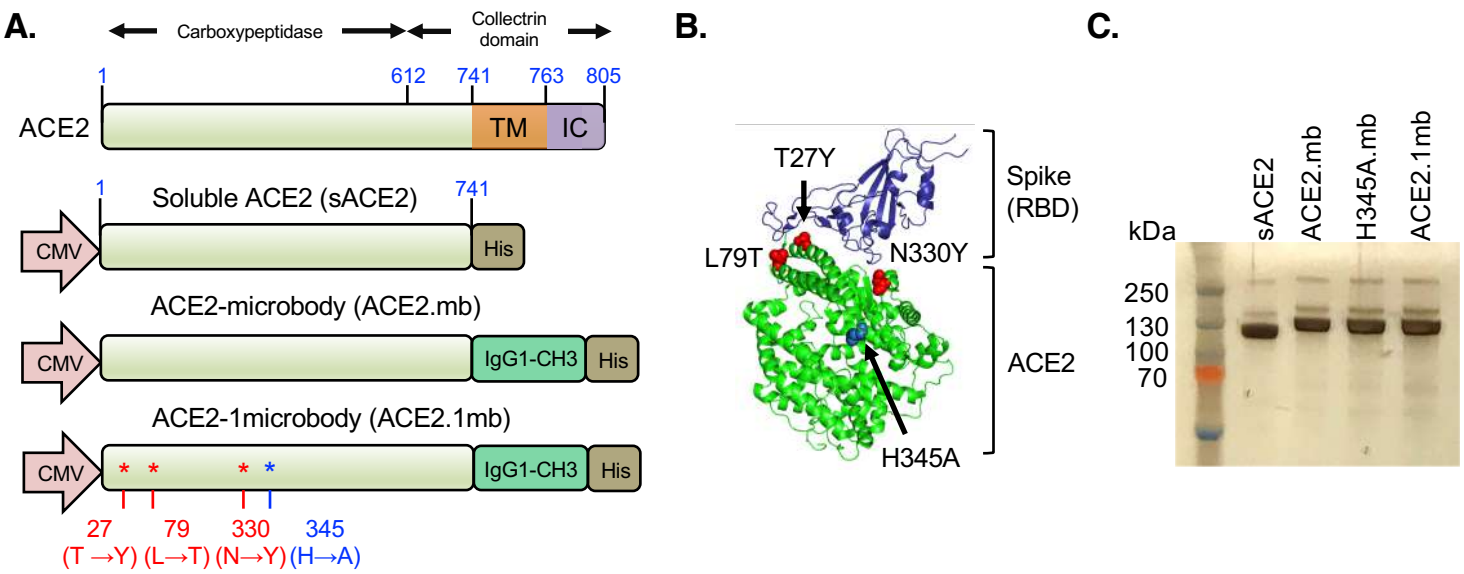

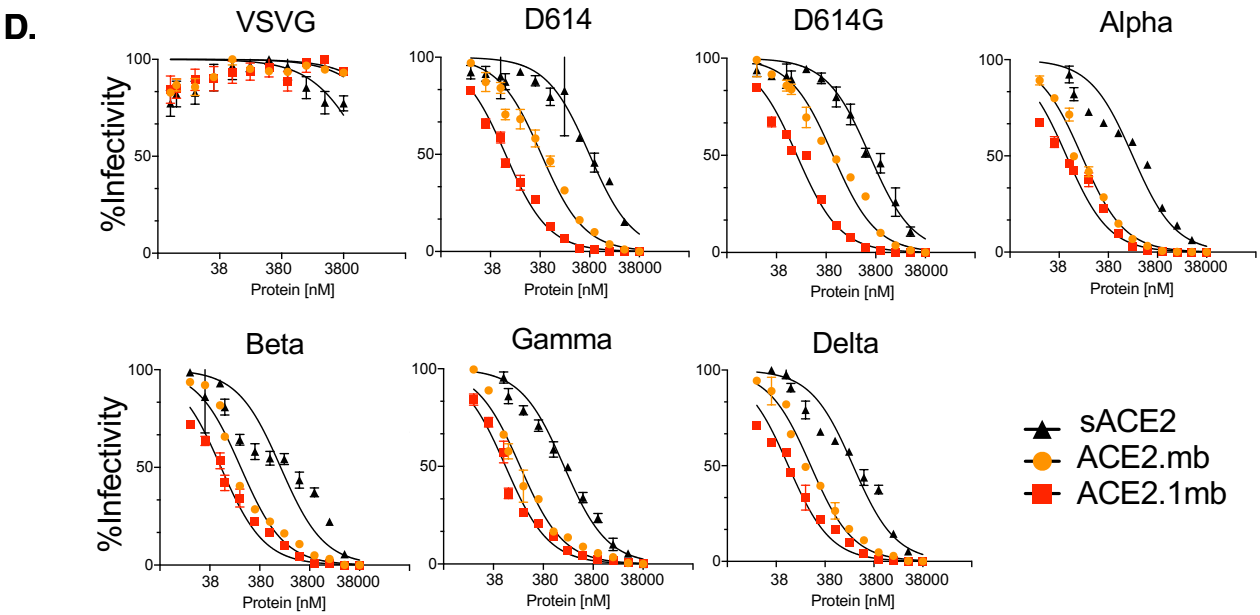

	IC50 (nM)						
	VSVG	D614	D614G	Alpha	Beta	Gamma	Delta
sACE2	ND	3,753	3,173	1,186	1,010	988	3,616
ACE2.mb	ND	402	523	109	158	130	391
ACE2.1mb	ND	76	98	54	65	67	100

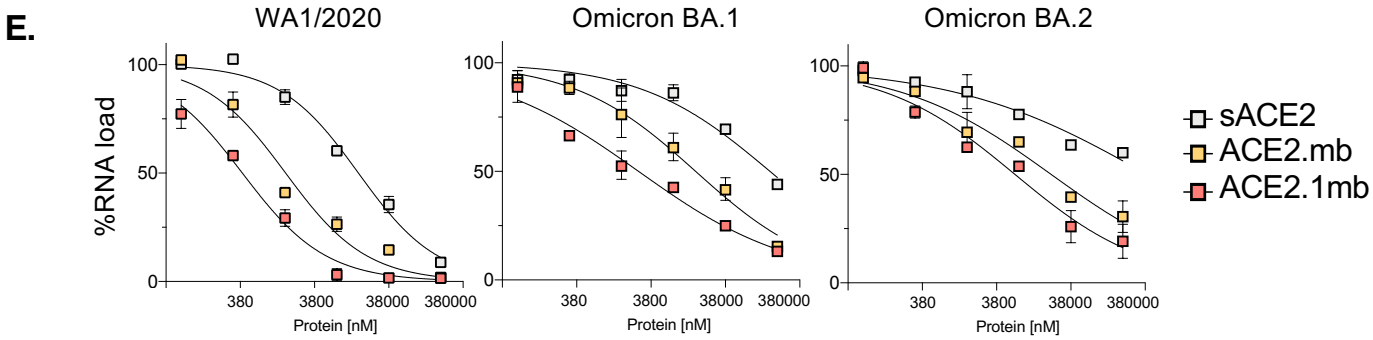

	IC50 (nM)		
	WA1/2020	Omicron BA.1	Omicron BA.2
sACE2	14,820	151,240	403,560
ACE2.mb	1,558	15,124	20,596
ACE2.1mb	418	2,584	6,726

Figure. 1

A.

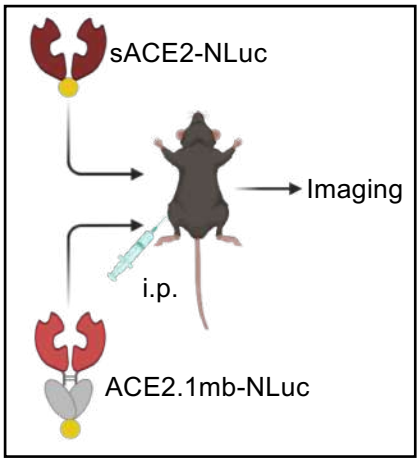

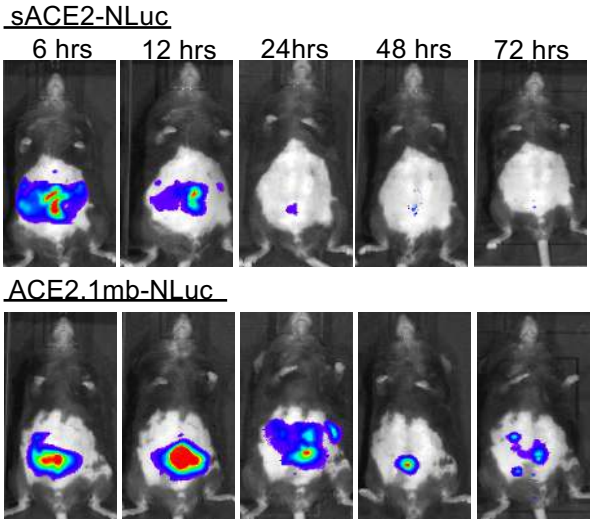

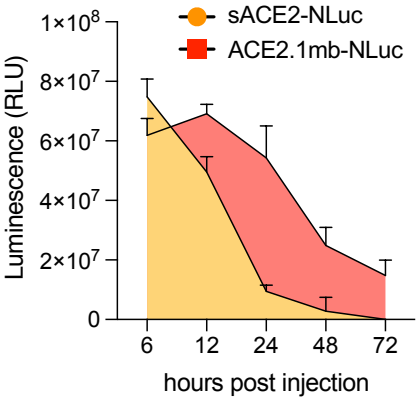

B.

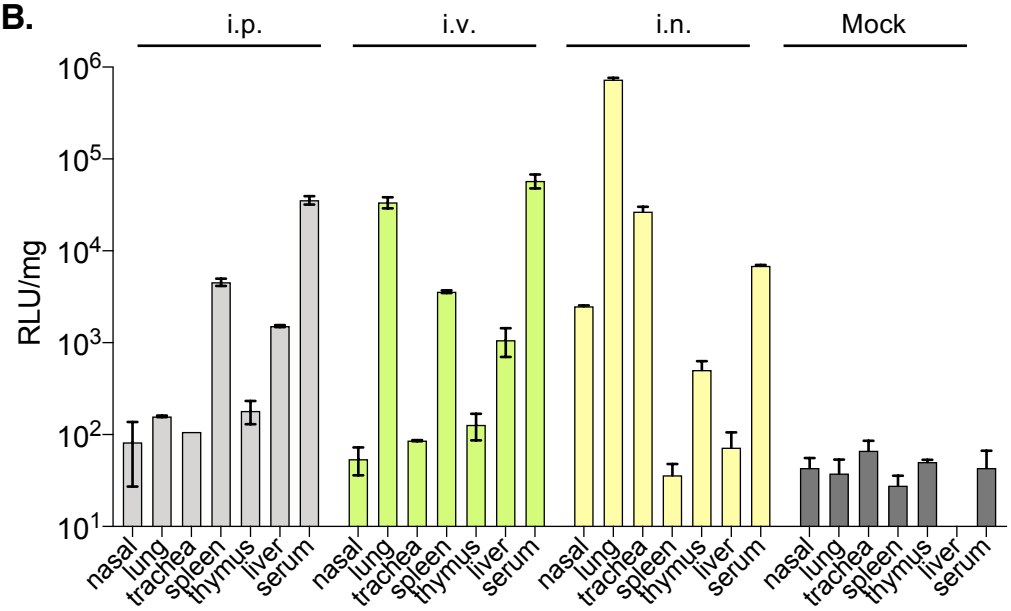

C.

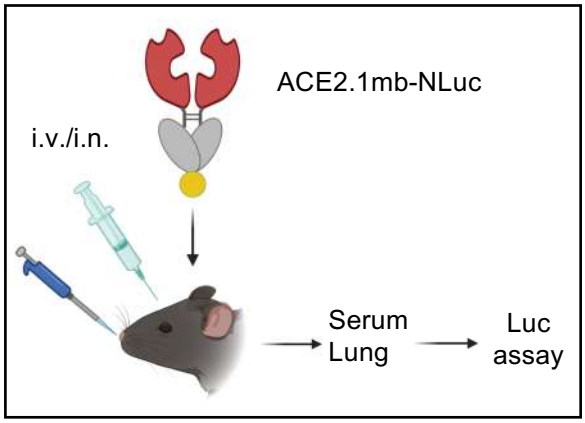

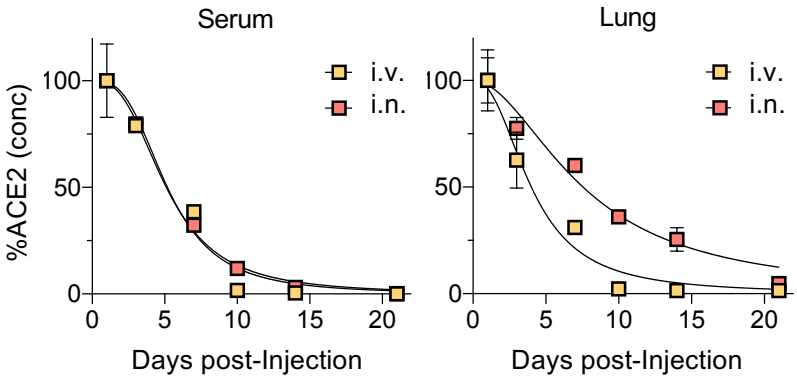

Serum		Lung	
i.v.	i.n.	i.v.	i.n.
5.2 days	5.1 days	4.0 days	7.6 days

Figure. 2

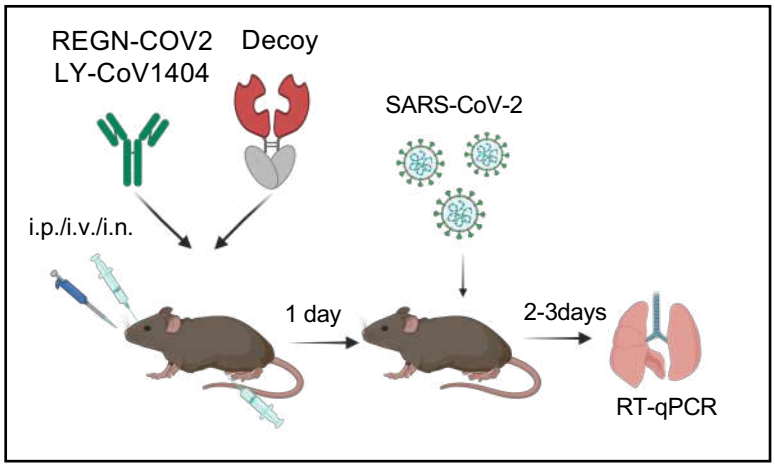
A.
REGN-COV2
LY-CoV1404
Decoy
SARS-CoV-2
i.p./i.v./i.n.
1 day
2-3days
RT-qPCR

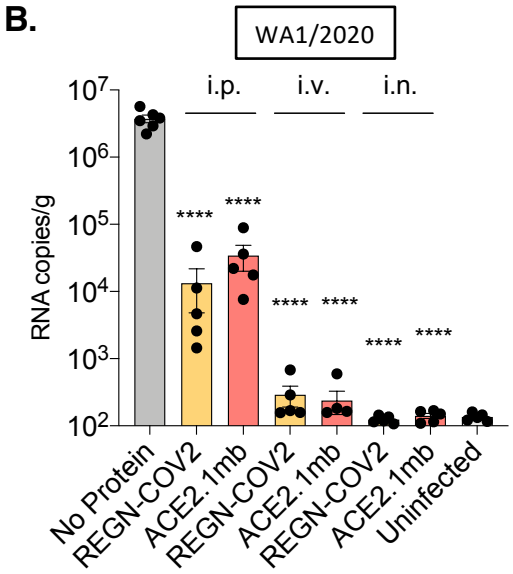
B.
WA1/2020
i.p.
i.v.
i.n.
RNA copies/g
No Protein
REGN-COV2
ACE2.1mb
REGN-COV2
ACE2.1mb
REGN-COV2
ACE2.1mb
Uninfected

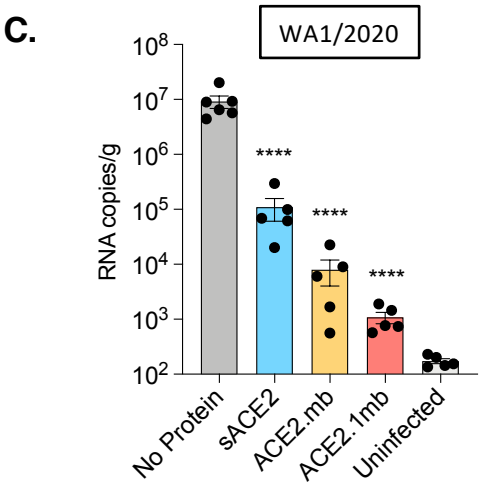
C.
WA1/2020
RNA copies/g
No Protein
sACE2
ACE2.mb
ACE2.1mb
Uninfected

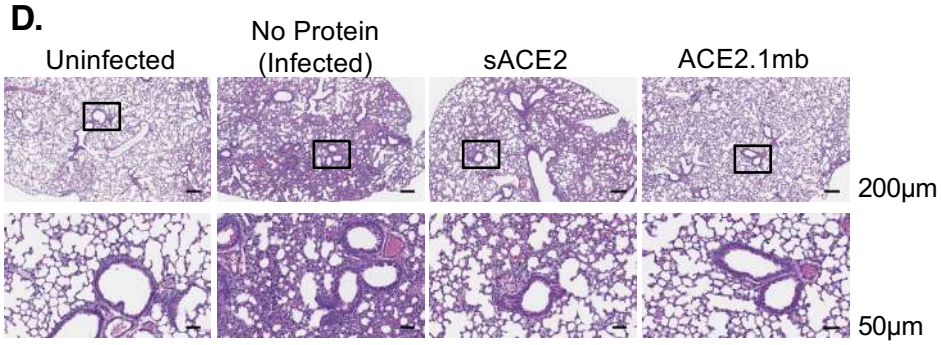
D.
Uninfected
No Protein
(Infected)
sACE2
ACE2.1mb
200μm
50μm

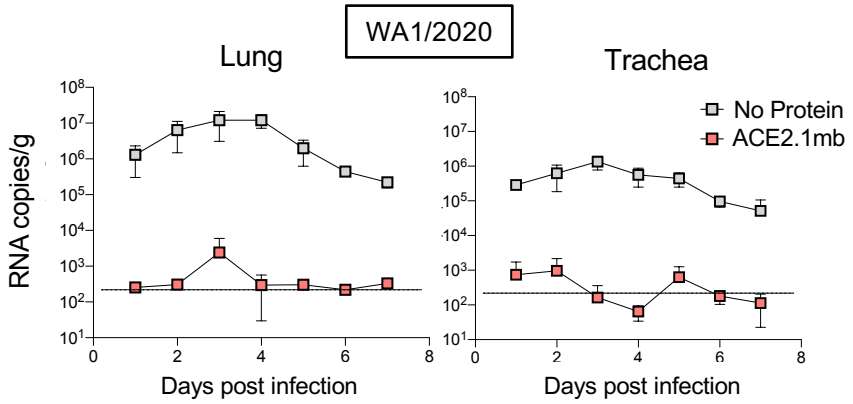
E.
WA1/2020
Lung
Trachea
No Protein
ACE2.1mb
RNA copies/g
Days post infection
Days post infection

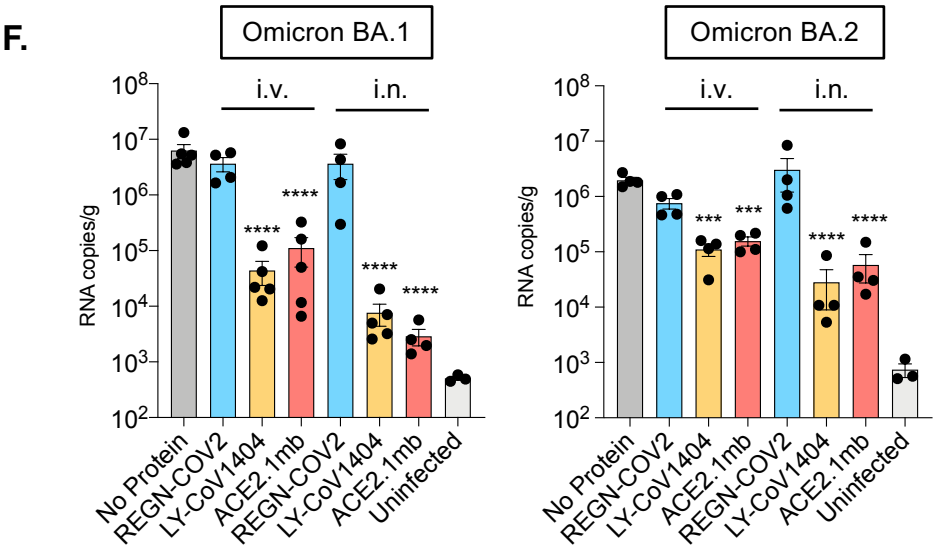
F.
Omicron BA.1
Omicron BA.2
i.v.
i.n.
RNA copies/g
No Protein
REGN-COV2
LY-CoV1404
ACE2.1mb
REGN-COV2
LY-CoV1404
ACE2.1mb
Uninfected

Figure. 3

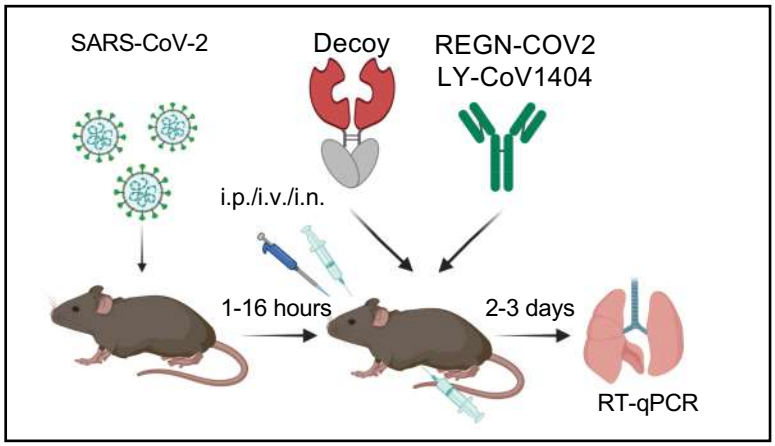
A.
SARS-CoV-2
Decoy
REGN-COV2
LY-CoV1404
i.p./i.v./i.n.
1-16 hours
2-3 days
RT-qPCR

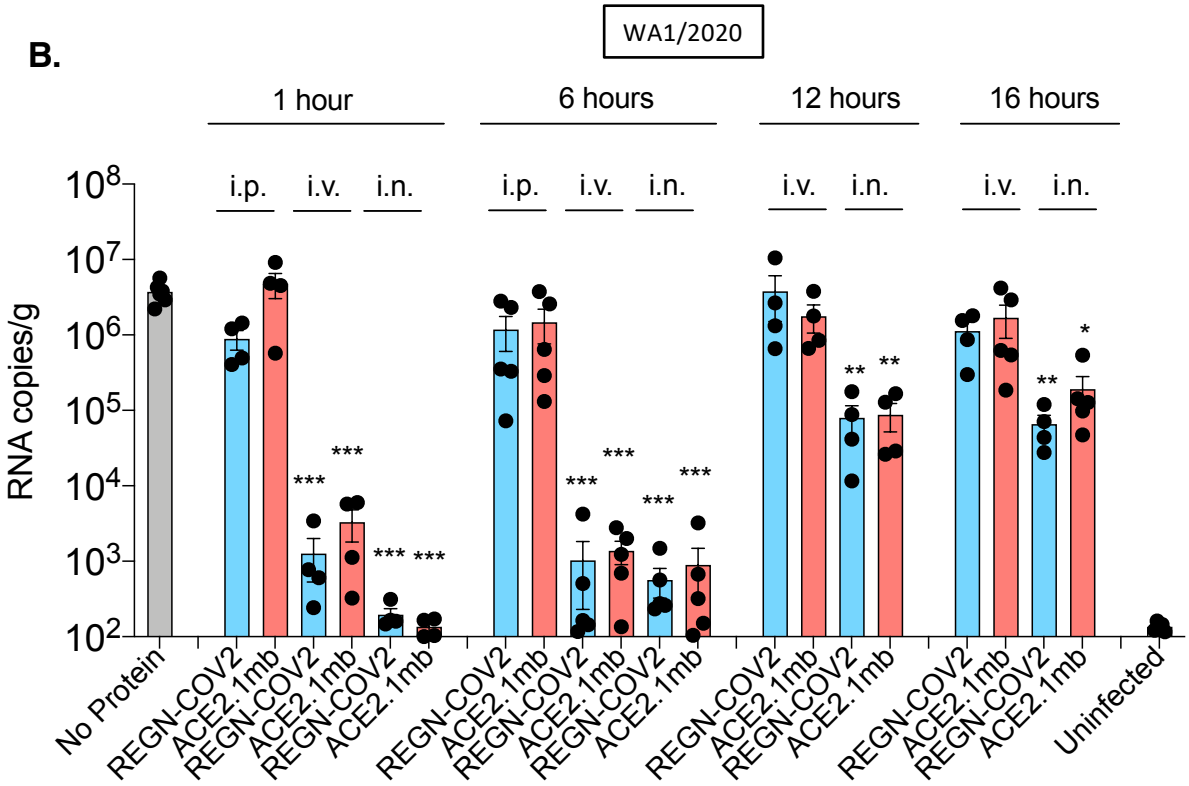
B.
WA1/2020
1 hour
6 hours
12 hours
16 hours
i.p.
i.v.
i.n.
RNA copies/g
No Protein
REGN-COV2
ACE2.1mb
Uninfected

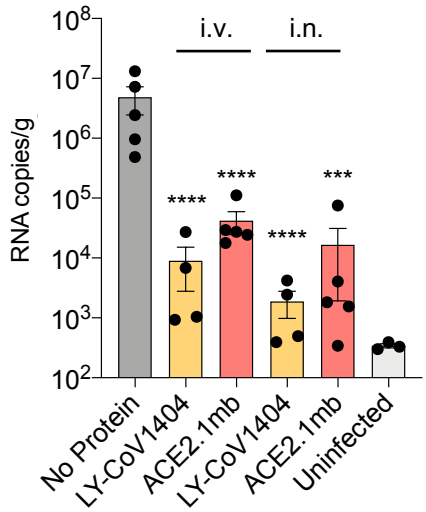
C.
Omicron BA.1
i.v.
i.n.
RNA copies/g
No Protein
LY-CoV1404
ACE2.1mb
Uninfected

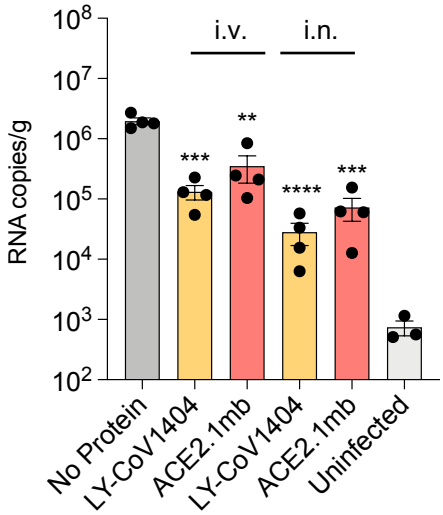
Omicron BA.2
i.v.
i.n.
RNA copies/g
No Protein
LY-CoV1404
ACE2.1mb
Uninfected

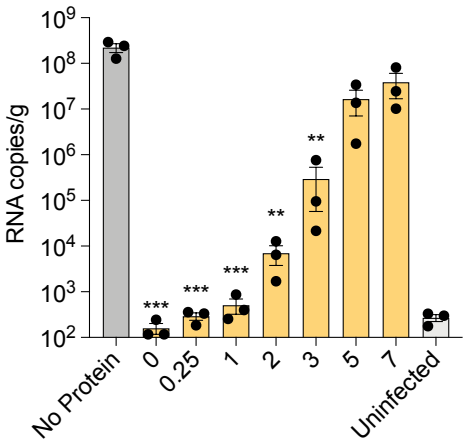
D.
RNA copies/g
No Protein
0
0.25
1
2
3
5
7
Uninfected

Figure. 4

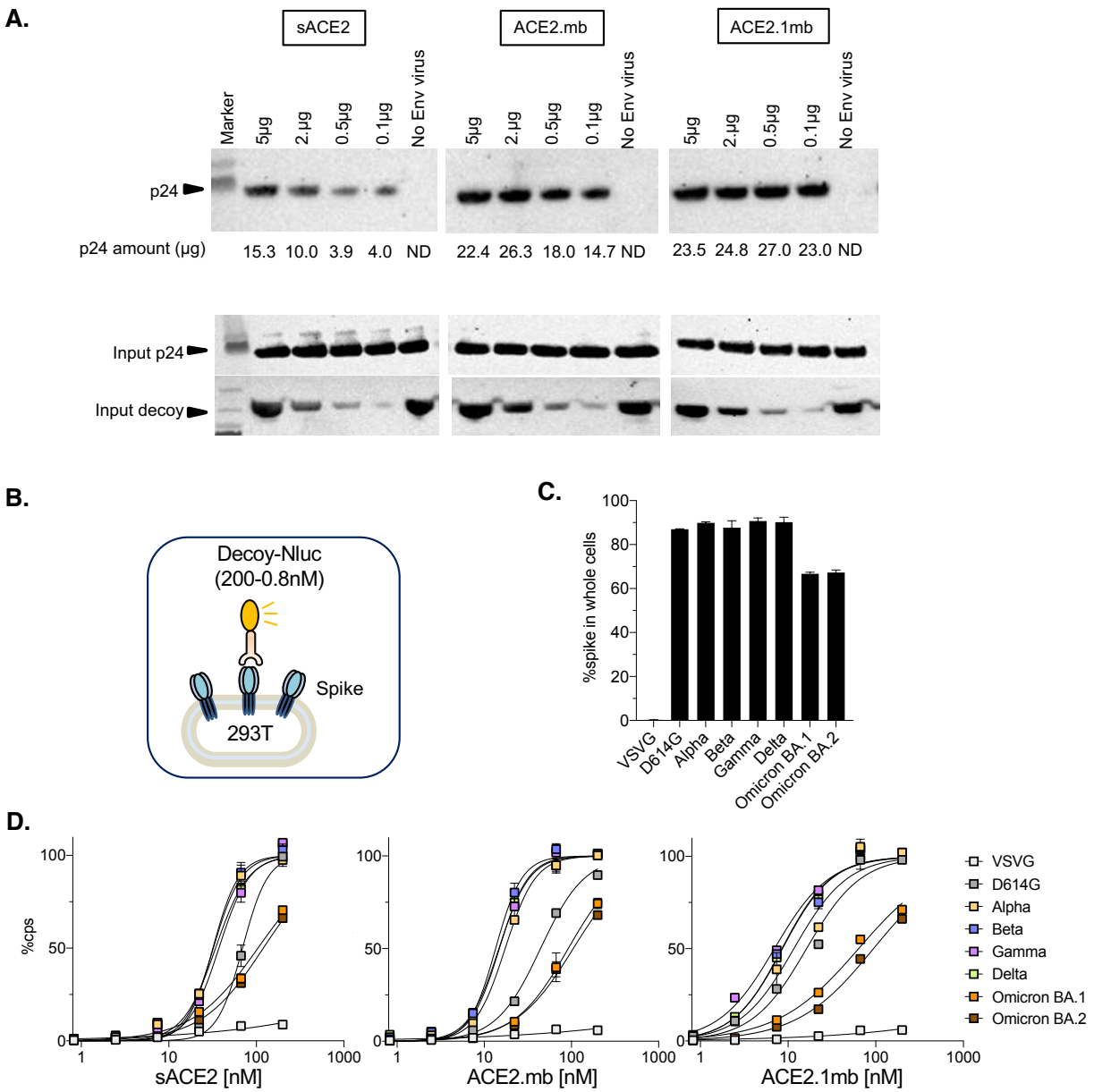

	50% binding (nM)							
	VSVG	D614G	Alpha	Beta	Gamma	Delta	Omicron BA.1	Omicron BA.2
sACE2	ND	69.48	32.25	31.87	37.35	34.18	104.1	120
ACE2.mb	ND	44.18	17.36	13.49	14.74	14.89	91.85	104.8
ACE2.1mb	ND	16.25	11.65	8.641	6.987	8.515	63.76	94.21

Supplementary Figure 1. Increased affinity of ACE2.1mb for the spike protein.

(A) Ni-NTA agarose beads were coated with different amounts (5, 2, 0.5, 0.1 µg) of sACE2, ACE2.mb or ACE2.1mb. A fixed amount of lentiviral virions pseudotyped with the D614G spike protein (30 µl) or control virions lacking the spike were incubated with the beads. After 1 hour,

free virions were removed by centrifugation and the remaining bead-bound virions were detected on an immunoblot probed with anti-p24 antibody. The amount of bead-bound p24 capsid protein was calculated against a standard curve with recombinant capsid and is indicated below each lane. Input virions and decoy proteins were detected on an immunoblot probed with anti-p24 and anti-His antibody and are shown below. ND: Not detected.

(B) The decoy:spike binding assay is diagrammed (left). 293T cells were transfected with 2 μg pcDNA-6 expression vectors for the VOC spike proteins. The cells were incubated at 37° with different amounts of decoy:luciferase fusion proteins. After 1 hour, unbound protein was removed by centrifugation and the amount of bound decoy protein was determined by luciferase assay. The amount of spike protein on the transfected 293T cells was analyzed by flow cytometry with anti-spike monoclonal antibody against the S2 protein (right). Avidity or the decoys is shown as curves with 100% binding set as luciferase activity at 400 nM decoy (below). The table shows the decoy concentration required for 50% maximal binding. The experiment was done three times with similar results.

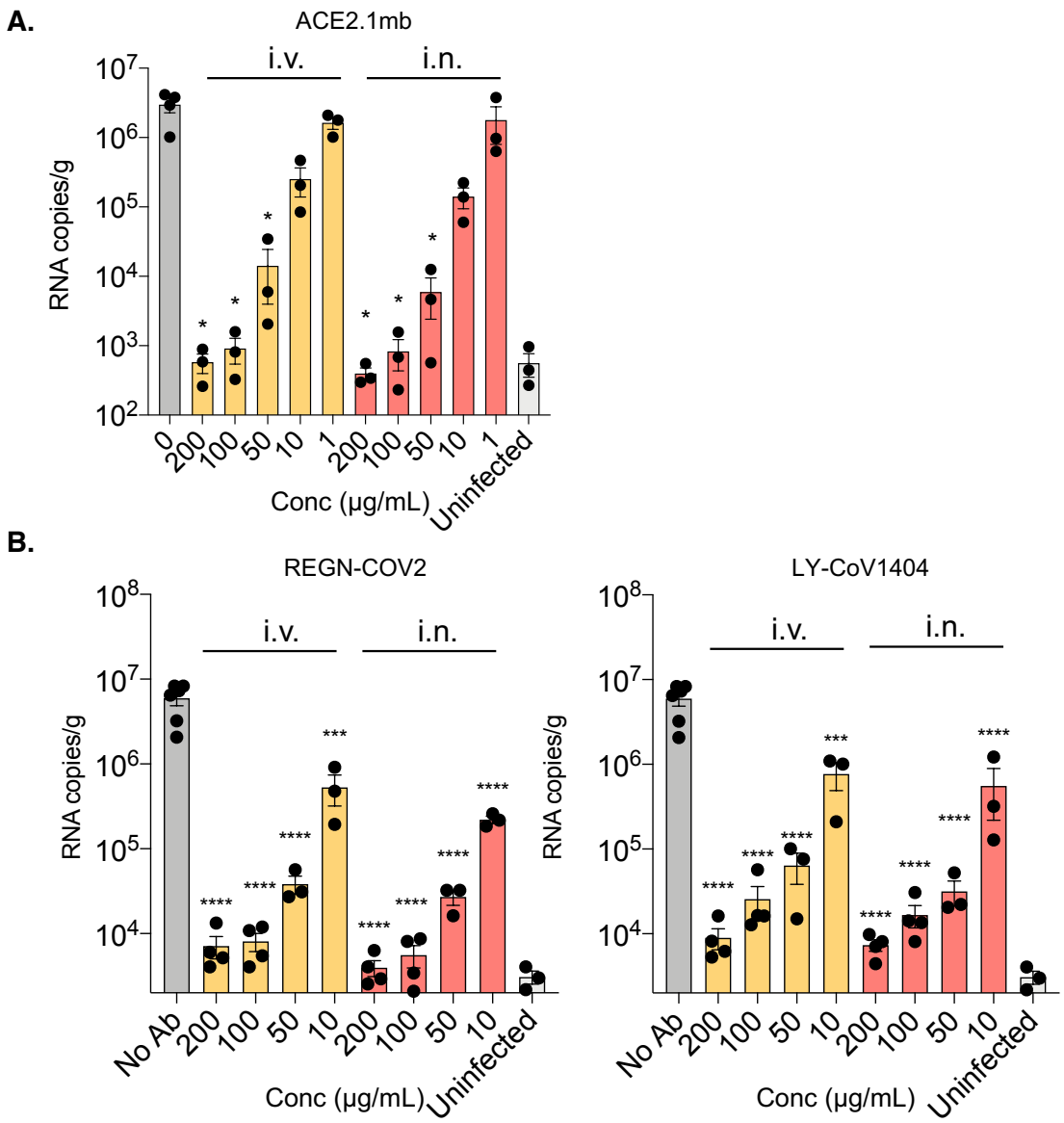

Supplementary Figure 2. Decoy and therapeutic monoclonal antibodies protect mice from SARS-CoV-2 infection.

(A) hACE2-Tg mice were injected i.v. or instilled i.n. with different amounts of decoy proteins. At 1-dpi, the mice were challenged with 1 X 10^4 PFU SARS-CoV-2 USA-WA1/2020 (n=3). Three days post-infection, lung subgenomic viral E RNA was quantified by RT-qPCR.

(B) hACE2-Tg mice were injected i.v. or instilled i.n. with different amounts of REGN-COV2 or LY-CoV1404 antibody (n=3). At 1-dpi, the mice were challenged with 1 X 10^4 PFU of SARS-CoV-2 USA-WA1/2020. At 3-dpi, lung subgenomic viral E RNA was quantified by RT-qPCR.